

PAPER

Effect of Coulomb repulsion on the London penetration depth in cuprate superconductors

To cite this article: K K Komarov and D M Dzebisashvili 2020 *Phys. Scr.* **95** 065806

View the [article online](#) for updates and enhancements.

Effect of Coulomb repulsion on the London penetration depth in cuprate superconductors

K K Komarov¹  and D M Dzebisashvili^{1,2} 

¹Kirensky Institute of Physics, Federal Research Center KSC SB RAS 660036, Krasnoyarsk, Russia

²Reshetnev Siberian State University of Science and Technology 660037, Krasnoyarsk, Russia

E-mail: constlike@gmail.com and ddm@iph.krasn.ru

Received 11 December 2019, revised 11 March 2020

Accepted for publication 19 March 2020

Published 18 May 2020



CrossMark

Abstract

We study the effect of Coulomb repulsion between oxygen holes on the London penetration depth λ based on the concept of spin-polaron nature of Fermi quasiparticles in cuprate superconductors. It is shown that for the generally accepted values of the parameters of the spin-fermion model, taking into account the Coulomb interaction, both the one-site Hubbard U_p and interaction between holes on the next-nearest-neighbor oxygen ions V_2 , allows one to achieve a much better agreement of the calculated temperature dependencies of the value λ^{-2} with the experimental data in $\text{La}_{2-x}\text{Sr}_x\text{CuO}_4$ in a wide range around optimal doping.

Keywords: strongly correlated electron systems, Mott-Hubbard materials, high-temperature superconductivity, spin-charge coupling, Coulomb repulsion, London penetration depth

(Some figures may appear in colour only in the online journal)

1. Introduction

The existence of strong electron correlations (SEC), due to the significant Coulomb interaction of holes in $d_{x^2-y^2}$ -orbitals of copper ions, essentially complicates the study of low-temperature properties of cuprate high-temperature superconductors (HTSC). On the other hand, it is the large value of this interaction that allows to integrate out the high-energy states in the, most realistic for cuprates, three-band $p-d$ model or the Emery model [1–5] and to obtain a more simple spin-fermion model (SFM) [6–10]. An important difference of the last model from the other effective low-energy models of cuprates, such as the Hubbard model (for example, [11, 12]) or the $t-J$ model [13], is that the SFM clearly takes into account the spatial separation of hole states on the copper ion and two oxygen ions in the unit cell of CuO_2 -planes.

Within SFM, the concept of a spin polaron was developed [14–16], which made it possible to achieve significant progress in describing the properties of cuprates both in the normal [16–21], and superconducting [22–24] phases. In particular, in [22–24] it was shown that the Cooper instability develops in an ensemble of spin polarons, and the exchange interaction

between the spins localized on copper ions causes an effective attraction between spin-polaron quasiparticles.

Recently, in [25], the spin polaron concept was used to describe the dependence of the London penetration depth λ on the temperature T in hole-doped cuprate HTSCs. An important result of these studies was the detection of the so-called inflection point in the calculated curves of $\lambda^{-2}(T)$, which was experimentally observed, for example, in $\text{La}_{1.83}\text{Sr}_{0.17}\text{CuO}_4$ [26, 27], $\text{YBa}_2\text{Cu}_3\text{O}_{7-\delta}$ [28, 29] and $\text{Bi}_{2.15}\text{Sr}_{1.85}\text{CaCu}_2\text{O}_{8+\delta}$ [30].

Unfortunately in [25] the theoretical curves $\lambda^{-2}(T)$ exceeded the experimental ones for the $\text{La}_{2-x}\text{Sr}_x\text{CuO}_4$ (LSCO) [31] by 30%–40%, both regarding the value of λ_0^{-2} (i.e. λ^{-2} at $T = 0$) and the value of T_c which is the temperature at which λ diverges. It is important to note that parameters of the SFM were not adjusted, but were chosen equal to those used earlier [18, 19, 21–24]. To obtain a satisfactory agreement of the $\lambda^{-2}(T)$ curves with the experimental data, it was necessary to reduce by almost two times both the parameter of the spin-fermion coupling J , which significantly affects the value of the superconducting current, and the super-exchange parameter I , which is the coupling constant in the spin-polaron ensemble, and thus, determining the critical temperature T_c . If the two-fold

reduction of J , used to fit the results in [25], could still be somehow justified (the effective parameter J depends on the parameters of the original Emery model and can vary within the specified limits), then the reduction of the exchange integral I was only illustrative.

In this work, it will be shown that taking into account the Coulomb repulsion between the holes on oxygen ions, eliminates the need to artificially underestimate the value of the super-exchange integral to achieve a satisfactory agreement between the theoretical and experimental temperature dependencies of the function $\lambda^{-2}(T)$ in cuprate HTSCs.

The paper is organized as follows. In the second section, SFM is formulated and necessary notations are introduced. The third section describes the modification of the SFM Hamiltonian, when the magnetic field is switched on, and the method of calculating the London length. In the fourth section, the projection method is briefly discussed, on the basis of which the spin polaron concept is implemented, and the system of equations for the Green's functions in the superconducting phase is given. The equations for the order parameter and spectrum of spin-polaron quasiparticles in the superconducting phase are discussed in section 5. Section 6 presents the results of numerical calculations of the function $\lambda^{-2}(T)$. The main conclusions of the paper are formulated in the final seventh section.

2. Spin-Fermion model

The following ratio between the parameters of the Emery model corresponds to the SEC regime in the cuprate HTSCs:

$$\Delta_{pd} \sim (U_d - \Delta_{pd}) \gg t_{pd} > 0, \quad (1)$$

where U_d is the Coulomb repulsion parameter of two holes on a copper ion, Δ_{pd} is the charge transfer gap between the hole states on copper and oxygen ions, and t_{pd} is the hybridization parameter between the d - and p -orbitals on copper and oxygen ions, respectively.

Inequalities (1) allow reducing the Emery model and obtaining SFM [6–10]. Using the quasi-momentum representation for Fermi operators we write the SFM Hamiltonian in the form [32]

$$\hat{H}_{\text{sp-f}} = \hat{H}_h + \hat{J} + \hat{I} + \hat{U}_p + \hat{V}_{pp}, \quad (2)$$

where

$$\begin{aligned} \hat{H}_h = & \sum_{k\alpha} (\xi_{k_x} a_{k\alpha}^\dagger a_{k\alpha} + \xi_{k_y} b_{k\alpha}^\dagger b_{k\alpha} \\ & + t_k (a_{k\alpha}^\dagger b_{k\alpha} + b_{k\alpha}^\dagger a_{k\alpha})), \end{aligned} \quad (3)$$

$$\hat{J} = \frac{J}{N} \sum_{\substack{f,k,q \\ \alpha,\beta}} e^{if(q-k)} u_{k\alpha}^\dagger (\vec{S}_f \vec{\sigma}_{\alpha\beta}) u_{q\beta}, \quad (4)$$

$$\hat{I} = \frac{I}{2} \sum_{f,\delta} \vec{S}_f \vec{S}_{f+\delta}, \quad (5)$$

$$\hat{U}_p = \frac{U_p}{N} \sum_{1,2,3,4} [a_{1\uparrow}^\dagger a_{2\downarrow}^\dagger a_{3\downarrow} a_{4\uparrow} + (a \rightarrow b)] \delta_{1+2-3-4}, \quad (6)$$

$$\begin{aligned} \hat{V}_{pp} = & \frac{4V_1}{N} \sum_{\substack{1,2,3,4 \\ \alpha,\beta}} \phi_{3-2} a_{1\alpha}^\dagger b_{2\beta}^\dagger b_{3\beta} a_{4\alpha} \delta_{1+2-3-4} \\ & + \frac{V_2}{N} \sum_{\substack{1,2,3,4 \\ \alpha,\beta}} [\theta_{2-3}^{xy} a_{1\alpha}^\dagger a_{2\beta}^\dagger a_{3\beta} a_{4\alpha} \\ & + \theta_{2-3}^{yx} (a \rightarrow b)] \delta_{1+2-3-4}. \end{aligned} \quad (7)$$

When writing (3)–(7) the following notations were used

$$\begin{aligned} \xi_{k_{x(y)}} = & \tilde{\xi}_p + 2\tau s_{k,x(y)}^2 - \mu, \quad \tilde{\xi}_p = \varepsilon_p + 2V_{pd}, \\ t_k = & (2\tau - 4t) s_{k,x} s_{k,y}, \quad s_{k,x(y)} = \sin(k_{x(y)}/2), \\ \phi_k = & \cos \frac{k_x}{2} \cdot \cos \frac{k_y}{2}, \quad \theta_k^{xy(yx)} = e^{ik_x(y)} + e^{-ik_y(x)}, \\ \tau = & t_{pd}^2 (1 - \eta) / \Delta_{pd}, \quad \eta = \Delta_{pd} / (U_d - \Delta_{pd} - 2V_{pd}), \\ J = & 4t_{pd}^2 (1 + \eta) / \Delta_{pd}, \quad u_{k\beta} = s_{k,x} a_{k\beta} + s_{k,y} b_{k\beta}. \end{aligned} \quad (8)$$

The \hat{H}_h operator describes holes on oxygen ions. $a_{k\alpha}^\dagger$ ($a_{k\alpha}$) denotes the hole creation (annihilation) operators with a quasi-momentum k and with a spin projection $\alpha = \pm 1/2$ in the oxygen ion subsystem with the p_x -orbitals. Similar operators from the oxygen ion subsystem with the p_y -orbitals are denoted by $b_{k\alpha}^\dagger$ ($b_{k\alpha}$). The parameter ε_p corresponds to the bare binding energy of the holes on oxygen ions. This energy is increased by $2V_{pd}$ taking into account the Coulomb interaction of the oxygen hole with the two nearest copper ions (V_{pd} is the value of this interaction). The integral of the hole hopping between the oxygen ions is denoted by t . The parameter τ is due to hybridization of the p - and d -orbitals on the copper and oxygen ions. μ is the chemical potential.

The \hat{U}_p operator defined by (6) describes the Hubbard repulsion of two holes on an oxygen ion with the intensity of U_p . For brevity, quasi-momenta and spins with the corresponding indices are denoted by numbers, for example: $1 \equiv \{k_1, \sigma_1\}$. The Kronecker symbol $\delta_{1+2-3-4}$ accounts for the momentum conservation law: $\delta_{k_1+k_2-k_3-k_4}$. N is the number of unit cells.

Intersite Coulomb interactions of the holes located at the nearest-neighbor and next-nearest-neighbor oxygen ions (figure 1) are described by the operator \hat{V}_{pp} (see (7)). The value of these interactions is determined by the parameters V_1 and V_2 , respectively. The functions ϕ_k and $\theta_k^{xy(yx)}$ appear in the transition from the Wannier representation to the quasi-momentum representation and take into account the crystal symmetry of the CuO_2 -plane.

The \hat{J} operator appears in the second order in the hybridization parameter t_{pd} and is defined by (4). This operator takes into account both the exchange interaction between the spins of the holes on copper and oxygen ions, and the spin-correlated hoppings of the hole in the oxygen subsystem with the simultaneous flipping of the localized spin. The spin on the copper ion with the site index f is described by the operator \vec{S}_f , and the vector $\vec{\sigma}$ in (4) is composed of the Pauli matrices: $\vec{\sigma} = (\sigma^x, \sigma^y, \sigma^z)$.

Finally, the \hat{I} operator takes into account the super-exchange interaction between the nearest-neighbor spins on copper ions and appears in the fourth order of the perturbation

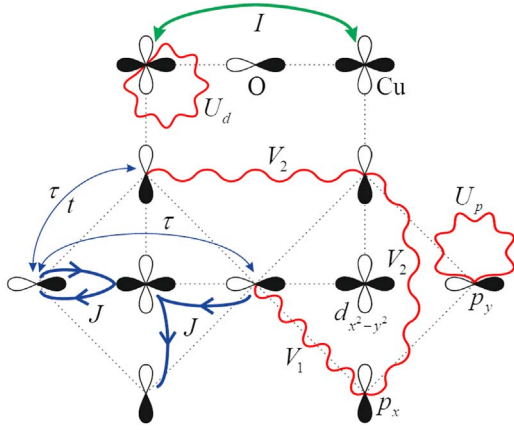


Figure 1. The structure of the CuO_2 -plane. Oxygen $p_x(p_y)$ orbitals and copper $d_{x^2-y^2}$ orbitals are shown. Wavy lines denote Coulomb interactions: $U_{p(d)}$ —on-site Coulomb repulsion of holes on an oxygen (copper) ion; V_1 and V_2 —intersite Coulomb interactions of the holes located at the nearest-neighbor and the next-nearest-neighbor oxygen ions, respectively. The bold green line with arrows stands for the super-exchange interaction (I) between spins on the nearest-neighbor copper ions. The bold blue lines next to the letter J correspond to both the spin-fermion exchange interaction and the spin-correlated hoppings. τ —effective hole hoppings arising due to p – d -hybridization in the second order of perturbation theory, t —the integral of direct hole hoppings between nearest oxygen ions (find τ and t near the thin blue line with arrows).

theory on the parameter t_{pd} . Vector δ in (5) connects the site f from the copper sublattice with four nearest sites from the same sublattice.

The SFM parameters—the effective hopping τ , the integrals of the p – d -exchange (J) and super-exchange (I) interactions—are expressed in terms of the parameters of the original Emery model (see, for example, [7]). The latter are obtained with satisfactory accuracy [33–35]. Taking this into account as well as the results in [21, 24], we have chosen the following values of the SFM parameters (in eV): $J = 1.76$, $I = 0.118$, $\tau = 0.225$, $U_p = 3$ [33]. The value of the Coulomb interaction parameters V_1 can be estimated in the range 1–2 eV [35] albeit, as will be shown below, the particular value of V_1 turns out not to be too significant for d-wave superconductivity. The value of V_2 we estimated within 0.1–0.2 eV according to [36]. For the oxygen-oxygen hopping integral we take $t = 0.12$ eV which is a reduced value as compared to the one usually used. For choosing this value of t we have at least two reasons following from our previous study of cuprate HTSC in both normal phase [21] and d-wave superconducting phase [24].

An important circumstance to be taken into account in the spin-polaron approach is that the localized spin subsystem is in the quantum spin-liquid state. This means that the long-range magnetic order is absent in the copper ion subsystem: $\langle S_f^\alpha \rangle = 0$ ($\alpha = x, y, z$), but short-range spin correlations remain. These correlations are taken into account through the spin correlation functions C_j , which are defined as thermodynamic average of the two spin operators located at a distance r_j : $C_j = \langle \vec{S}_f \vec{S}_{f+r_j} \rangle$, where j is the number of the coordination sphere of the site f .

In the spin-liquid phase, these correlators satisfy the sequence of equalities: $C_j = 3 \langle S_f^x S_{f+r_j}^x \rangle = 3 \langle S_f^y S_{f+r_j}^y \rangle = 3 \langle S_f^z S_{f+r_j}^z \rangle$. In the low temperature range ($\lesssim 100$ K) the spin correlators are almost independent of temperature, but strongly depend on the doping x . The correlators C_j as functions of x were calculated, for example, in [37] based on the frustrated Heisenberg model on a square lattice in the framework of the spherically symmetric approach [38]. The values of C_j (with $j = 1, 2, 3$) used for different x were taken from [19].

3. The London penetration depth

Calculation of the penetration depth of the magnetic field λ in superconductors is based on the London equation: $\vec{j} = -c/(4\pi\lambda^2)\vec{A}$, where c is the speed of light. In the local approximation this equation establishes a relation between the superconducting current density \vec{j} and the vector potential of the magnetic field \vec{A} , and the proportionality coefficient between them is determined by the value of λ . To calculate the superconducting current density \vec{j} in an ensemble of spin-polaron quasiparticles we should include into Hamiltonian (2) terms accounting for coupling to the magnetic field. This can be done via Peierls substitution [39, 40]. Considering vector potential \vec{A}_q in the long-wavelength limit: $q = 0$ [41, 42] we find [25] that Hamiltonian (2) acquires an additional phase

$$\alpha_x = \frac{eg_x}{2c\hbar} A_{q=0}^x \quad (9)$$

in the argument of the trigonometric function $s_{k,x}$ (8). Here g_x is the lattice constant and for simplicity, we directed the vector potential along the x -axis.

Thus, a new definition of the function $s_{k,x}$, which takes into account the magnetic field, has the form:

$$s_{k,x} = \sin(k_x/2 - \alpha_x).$$

It is this definition for $s_{k,x}$ which will be used further. The function u_k which is linearly related to $s_{k,x}$ also apparently changes (see (8)). The function $s_{k,y}$ remains unchanged since in this case $A_{q=0}^y = 0$. The Zeeman energy determined by the spin moments of the holes is not taken into account because in the long wavelength limit ($q \rightarrow 0$) this energy tends to zero.

The resulting expression for the average value of the superconducting current density, obtained in [25] within SFM, is as follows:

$$j_x(q=0) = \frac{eg_x}{\hbar} \sum_{k\alpha} \cos\left(\frac{k_x}{2} - \alpha_x\right) [2\tau s_{k,x} \langle a_{k\alpha}^\dagger a_{k\alpha} \rangle + (2\tau - 4t) s_{k,y} \langle a_{k\alpha}^\dagger b_{k\alpha} \rangle + J \langle a_{k\alpha}^\dagger L_{k\alpha} \rangle], \quad (10)$$

where expressions for thermodynamic averages in square brackets are given in the appendix by (A.7). Expression (10), in particular, gives the correct behavior of the current density at $T \geq T_c$. Indeed, in the normal phase the dependence of all thermodynamic averages (A.7) on the quasi-momentum k_x is determined only as the difference $k_x - \alpha_x$. Therefore, a simple substitution of the integration variable $k_x \rightarrow k_x + \alpha_x$

in the integral in the right part of the expression (10) allows one to eliminate the phase α_x . Since for $\alpha_x = 0$ the integrand in (10) is antisymmetric to \vec{k} , the right part of (10), as required, vanishes.

In the superconducting phase (for $T < T_c$), the dependence of the thermodynamic averages on k_x is determined both by the difference $k_x - \alpha_x$ and by the sum of $k_x + \alpha_x$. In this case, the integral in (10) is nonzero.

The inverse square of penetration depth λ^{-2} was determined numerically according to the London equation at $T < T_c$ as

$$\frac{1}{\lambda^2} = -\frac{4\pi}{c} \cdot \frac{j_x(q=0)}{A_{q=0}^x},$$

where supercurrent density $j_x(q=0)$ is defined by (10).

The described approach for calculating λ is a sufficiently effective one, especially for multi-band systems, for which the analytical dependence of the quasiparticle spectrum on the quasi-momentum is unknown and can only be obtained numerically. The proposed approach is also convenient since there is no need to carry out cumbersome calculations connected with extracting paramagnetic and diamagnetic parts of the supercurrent density.

4. Equations for Green's functions

A significant feature of the Hamiltonian of the SFM (2) is a large value of the p - d -exchange interaction constant J , which greatly exceeds the values of all the other parameters of the model. This means that in calculating the energy structure of spin-polaron excitations and analyzing the conditions for superconducting pairing, one has to take into account this interaction exactly. An approach taking into consideration this strong p - d -exchange coupling and within which the corresponding spin-polaron quasiparticle appears is called the spin-polaron approach. For the particular implementation of this approach the Zwanzig-Mori projection technique has proved to be rather convenient [43–50].

According to the projection technique, first of all, it is necessary to introduce a minimal set of basis operators that allow one to correctly describe the quasiparticle excitations in the system. For the correct account of the strong spin-charge coupling in the SFM of interest, it is important to introduce into the specified basis, along with the bare hole operators $a_{k\alpha}$ and $b_{k\alpha}$, the operator

$$L_{k\alpha} = \frac{1}{N} \sum_{fj\beta} e^{if(q-k)} (\vec{S}_f \vec{\sigma}_{\alpha\beta}) u_{q\beta},$$

arising in the right part of the equations of motion for $a_{k\alpha}$ and $b_{k\alpha}$. As was shown in [14–16, 19] the three operators $a_{k\alpha}$, $b_{k\alpha}$ and $L_{k\alpha}$ are sufficient to describe spectral properties of Fermi excitations of the cuprate HTSCs in the normal phase. To analyze the conditions for Cooper instability the mentioned set of three operators, is necessary to be enlarged by three extra operators: $a_{-k\bar{\alpha}}^\dagger$, $b_{-k\bar{\alpha}}^\dagger$, $L_{-k\bar{\alpha}}^\dagger$ ($\bar{\alpha} = -\alpha$) [22–24], giving an opportunity to introduce anomalous thermodynamic averages.

The next step of the projection technique is to project the equations of motion for the basis operators (or for the corresponding Green's functions) on the original set of basis operators. The application of this method to the SFM (2) with the above basis of six operators is described in [19, 22, 32]. Omitting the details of the calculations, we give the answer for a closed system of equations for the Green's functions ($j = 1, 2, 3$):

$$\begin{aligned} (\omega - \xi_x)G_{1j} &= \delta_{1j} + t_k G_{2j} + J_x G_{3j} + \Delta_{1k} F_{1j} + \Delta_{2k} F_{2j}, \\ (\omega - \xi_y)G_{2j} &= \delta_{2j} + t_k G_{1j} + J_y G_{3j} + \Delta_{3k} F_{1j} + \Delta_{4k} F_{1j}, \\ (\omega - \xi_L)G_{3j} &= \delta_{3j} K_k + (J_x G_{1j} + J_y G_{2j}) K_k + \frac{\Delta_{5k}}{K_k} F_{3j}, \\ (\omega + \xi_x)F_{1j} &= \Delta_{1k}^* G_{1j} + \Delta_{3k}^* G_{2j} - t_k F_{2j} + J_x F_{3j}, \\ (\omega + \xi_y)F_{2j} &= \Delta_{2k}^* G_{1j} + \Delta_{4k}^* G_{2j} - t_k F_{1j} + J_y F_{3j}, \\ (\omega + \xi_L)F_{3j} &= \frac{\Delta_{5k}^*}{K_k} G_{3j} + (J_x F_{1j} + J_y F_{2j}) K_k. \end{aligned} \quad (11)$$

Here, for the normal and anomalous Green's functions, we use the short notations G_{ij} and F_{ij} , respectively. The meaning of these designations is revealed by the equalities:

$$\begin{aligned} G_{11} &= \langle\langle a_{k\uparrow} | a_{k\uparrow}^\dagger \rangle\rangle_\omega, & F_{11} &= \langle\langle a_{-k\downarrow}^\dagger | a_{k\uparrow}^\dagger \rangle\rangle_\omega, \\ G_{21} &= \langle\langle b_{k\uparrow} | a_{k\uparrow}^\dagger \rangle\rangle_\omega, & F_{21} &= \langle\langle b_{-k\downarrow}^\dagger | a_{k\uparrow}^\dagger \rangle\rangle_\omega, \\ G_{31} &= \langle\langle L_{k\uparrow} | a_{k\uparrow}^\dagger \rangle\rangle_\omega, & F_{31} &= \langle\langle L_{-k\downarrow}^\dagger | a_{k\uparrow}^\dagger \rangle\rangle_\omega. \end{aligned}$$

The functions $G_{i2}(F_{i2})$ and $G_{i3}(F_{i3})$ ($i = 1, 2, 3$) are defined in a similar way except for the operator $a_{k\uparrow}^\dagger$ being substituted for $b_{k\uparrow}^\dagger$ and $L_{k\uparrow}^\dagger$, respectively. When writing the system (11) we use the functions:

$$\begin{aligned} \xi_{x(y)} &= \xi_{k_{x(y)}}, & J_{x(y)} &= J s_{k,x(y)}, \\ \xi_L(k) &= \tilde{\xi}_p - \mu - 2t + 5\tau/2 - J - \tau C_1 \gamma_{1k}/2 \\ &+ [(\tau - 2t)(-C_1 \gamma_{1k} + C_2 \gamma_{2k}) + \tau C_3 \gamma_{3k}/2 \\ &+ J C_1 (1 + 4\gamma_{1k})/4 - I C_1 (\gamma_{1k} + 4)]/K_k, \end{aligned} \quad (12)$$

where

$$K_k = \langle\langle L_{k\uparrow}, L_{k\uparrow}^\dagger \rangle\rangle = 3/4 - C_1 \gamma_{1k}, \quad (13)$$

and γ_{jk} ($j = 1, 2, 3$) denote the square lattice invariants:

$$\begin{aligned} \gamma_{1k} &= (\cos(k_x - 2\alpha_x) + \cos k_y)/2, \\ \gamma_{2k} &= \cos(k_x - 2\alpha_x) \cos k_y, \\ \gamma_{3k} &= (\cos(2k_x - 4\alpha_x) + \cos 2k_y)/2, \end{aligned} \quad (14)$$

taking into account the magnetic field through the phase α_x .

The components of the superconducting order parameter Δ_{jk} are defined as anomalous thermodynamic averages:

$$\begin{aligned} \Delta_{1k} &= \langle\langle [a_{k\uparrow}, \hat{H}_{\text{sp-f}}], a_{-k\downarrow} \rangle\rangle, \\ \Delta_{2k} &= \langle\langle [a_{k\uparrow}, \hat{H}_{\text{sp-f}}], b_{-k\downarrow} \rangle\rangle, \\ \Delta_{3k} &= \langle\langle [b_{k\uparrow}, \hat{H}_{\text{sp-f}}], a_{-k\downarrow} \rangle\rangle, \\ \Delta_{4k} &= \langle\langle [b_{k\uparrow}, \hat{H}_{\text{sp-f}}], b_{-k\downarrow} \rangle\rangle, \\ \Delta_{5k} &= \langle\langle [L_{k\uparrow}, \hat{H}_{\text{sp-f}}], L_{-k\downarrow} \rangle\rangle. \end{aligned} \quad (15)$$

5. Equations for the superconducting order parameters and spin-polaron spectrum

The equations for the components of the superconducting order parameter Δ_{jk} ($j = 1, \dots, 5$) are obtained after calculating the commutators (and anticommutators) in the right hand part of formulas (15) and projecting the result of the calculations on the introduced basis of six operators. Since, according to the results of [32], the s-wave superconductivity in the SFM does not occur, when writing equations for Δ_{jk} , we keep only those terms which correspond to the d-wave pairing. The result is given in the appendix by (A.1). The components Δ_{2k} and Δ_{3k} for the d-wave pairing turn out to be zero. It is important to note that in the expressions (A.1) for Δ_{jk} the Coulomb repulsion parameter between the holes located on the nearest-neighbor oxygen ions V_1 is missing, since according to [51, 52] it should not contribute to the d-wave pairing.

Anomalous thermodynamic averages in the system of equations (A.1) are calculated using the spectral theorem [53] and corresponding Green's functions of the system (11). To analyze the conditions for Cooper instability, it is sufficient to calculate the anomalous averages in the linear approximation with respect to the components Δ_{jk} . As a result, a closed set of homogeneous integral equations for the components of the superconducting order parameter Δ_{jk}^* ($l = 1, 4, 5$) is obtained as follows

$$\begin{aligned} \Delta_{1k}^* &= -(\cos k_x - \cos k_y) \frac{2V_2}{N} \sum_{lq} \cos q_x M_{11}^{(l)}(q) \Delta_{lq}^*, \\ \Delta_{4k}^* &= -(\cos k_x - \cos k_y) \frac{2V_2}{N} \sum_{lq} \cos q_x M_{22}^{(l)}(q) \Delta_{lq}^*, \\ \Delta_{5k}^* &= +(\cos k_x - \cos k_y) \frac{I}{N} \sum_{lq} (\cos q_x - \cos q_y) \\ &\quad \times (M_{33}^{(l)}(q) - C_1 M_{uu}^{(l)}(q)) \Delta_{lq}^* \\ &\quad + \frac{U_p}{N} \sum_{lq} C_1 (\cos(k_x - 2\alpha_x) M_{11}^{(l)}(q) \\ &\quad + \cos k_y M_{22}^{(l)}(q)) \Delta_{lq}^* \\ &\quad - (\cos k_x - \cos k_y) \frac{2V_2}{N} \sum_{lq} C_1 \cos q_x \\ &\quad \times (M_{11}^{(l)}(q) + M_{22}^{(l)}(q)) \Delta_{lq}^*. \end{aligned} \quad (16)$$

When writing (16) we introduced the following functions

$$\begin{aligned} M_{uu}^{(l)}(q) &= -s_{q,x}^2 M_{11}^{(l)}(q) - s_{q,y}^2 M_{22}^{(l)}(q) \\ &\quad - s_{q,x} s_{q,y} (M_{12}^{(l)}(q) + M_{21}^{(l)}(q)), \end{aligned} \quad (17)$$

$$\begin{aligned} M_{nm}^{(l)}(q) &= \sum_{j=1,4} \frac{f(-E_{jq})}{2(-1)^{j+1} E_q (E_{jq} - \epsilon_{2q}) (E_{jq} - \epsilon_{3q})} \\ &\quad \times \frac{S_{nm}^{(l)}(q, E_{jq})}{(E_{jq} + \epsilon_{2,-q}) (E_{jq} + \epsilon_{2,-q})}, \end{aligned} \quad (18)$$

where $f(E) = 1/(\exp\{E/T\} + 1)$ is the Fermi-Dirac distribution function, ϵ_{jk} and E_{jk} are the energies of quasiparticles in the normal and superconducting states, respectively and $S_{ij}^{(l)}(k, \omega)$ are functions defined in the appendix (A.3).

The spectrum of Fermi excitations in the normal phase consists of three branches ϵ_{jk} ($j = 1, 2, 3$) and is determined from the solution of the third order dispersion equation

$$\begin{aligned} \det_k(\omega) &= +(\omega - \xi_x)(\omega - \xi_y)(\omega - \xi_L) \\ &\quad - 2J_x J_y t_k K_k - (\omega - \xi_y) J_x^2 K_k \\ &\quad - (\omega - \xi_x) J_y^2 K_k - (\omega - \xi_L) t_k^2 = 0, \end{aligned} \quad (19)$$

following from condition of existence of nontrivial solution of the system (11) at $\Delta_{jk} = 0$. With the doping levels x typical for cuprates, the dynamics of the holes on oxygen ions is determined solely by the lower band with the dispersion ϵ_{1k} . This branch of the spectrum is characterized by a minimum in the vicinity of $(\pi/2, \pi/2)$ point of the Brillouin zone and is significantly separated from the two upper branches ϵ_{2k} and ϵ_{3k} . The appearance of the lower branch is due to the strong spin-charge coupling, which induces an exchange interaction between the holes and localized spins at the nearest copper ions, as well as spin-correlated hoppings. The features of the spectrum ϵ_{1k} without magnetic field were discussed in [22]. In our case, taking into account the magnetic field is of fundamental importance.

Since the chemical potential μ in the systems under consideration lies in the lower band with the dispersion ϵ_{1k} , and the upper bands, as was mentioned above, are separated by a large energy gap, the spectra ϵ_{2k} and ϵ_{3k} are almost unchanged with transition to the superconducting phase: i.e. $E_{jk} = \epsilon_{jk}$ for $j = 2, 3$. Obtaining an expression for the spectrum E_{1k} for the lower spin-polaron band in the superconducting phase and in the weak magnetic field is described in detail in [54]. The expression for the spectrum E_{1k} has the form

$$E_{1k} = \delta\epsilon_{1k} + \sqrt{\epsilon_{1k}^2 + \Delta_k^2}, \quad (20)$$

where $\delta\epsilon_{1k}$ is a correction to the polaron spectrum in the normal phase ϵ_{1k} , which is antisymmetric in k and linear in α_x , and the gap function Δ_k^2 is expressed as a sum of squares of the components of the superconducting order parameter

$$\Delta_k^2 = |\Delta_{1k}|^2 + |\Delta_{4k}|^2 + |\Delta_{5k}|^2 / K_k^2. \quad (21)$$

Note that formally, in the sum over j in the right hand side of expression (18) it is necessary to take into account all the bands. However, since the upper bands (with $j = 2, 3$) are empty, their contributions can be ignored. The value of the index $j = 4$ in the sum over j in (18) corresponds to the spectrum $E_{4k} = -E_{1,-k}$.

One can see from the system of equations (16) that the kernels of the integral equations are split, and the solutions of this system are to be found in the following form

$$\begin{aligned} \Delta_{1k} &= B_{11}(\cos k_x - \cos k_y), \\ \Delta_{4k} &= B_{41}(\cos k_x - \cos k_y), \\ \Delta_{5k} &= B_{51} \cos k_x + B_{52} \cos k_y + B_{53}(\cos k_x - \cos k_y) \\ &\quad + B_{54}(\cos k_x - \cos k_y), \end{aligned} \quad (22)$$

where the six amplitudes B_{ij} determine the contribution of the corresponding basis functions to the expansion of the order parameter components.

Substituting expansion (22) into equations (16) and equating the factors of the corresponding trigonometric functions, we obtain a system of six algebraic equations for determining the amplitudes B_{ij} . It is also necessary to add to this system an equation for self-consistently finding the chemical potential μ :

$$x = \frac{2}{N} \sum_k \sum_{j=1,4} \frac{f(E_{jk})}{(-1)^{j+1} 2E_k(E_{jk} - \varepsilon_{2k})(E_{jk} - \varepsilon_{3k})} \times \frac{R^x(k, E_{jk})}{(E_{jk} + \varepsilon_{2,-k})(E_{jk} + \varepsilon_{3,-k})}, \quad (23)$$

where the function $R^x(k, \omega)$ is given in (A.5).

Numerical calculations show that the following relations between the amplitudes hold: $B_{11} = B_{41} \approx -B_{51} = B_{52}$, $B_{54}/B_{51} \approx -10$, $B_{54}/B_{53} \approx -10^2$. Thus, it is seen that the largest contribution to the order parameter component Δ_{5k} gives the amplitude B_{54} , proportional to the exchange integral I . Regarding this exchange integral, it should be noted that its value depends on the doping x . In [19], when calculating the exchange integral in the framework of the Heisenberg model, the effect of doping was simulated by the frustration of the exchange couplings. In accordance with [19], we used the product $I(1-p)$ as the exchange integral, where p is the frustration parameter varying from 0.15 to 0.275 with x increasing from 0.03 to 0.22.

6. Results and discussion

Calculations of the temperature dependence of the magnetic penetration depth λ taking into account the one-site Hubbard repulsion of holes and the Coulomb interaction between holes on the next-nearest-neighbor oxygen ions were carried out numerically based on expression (10) and self-consistent solution of the system of algebraic equations for the amplitudes B_{ij} together with chemical potential equation (23). It is important to note that, except for t , the rest of the Emery model parameters were chosen to be equal to those that are generally accepted for hole-doped cuprate HTSCs.

The calculation results are presented in figure 2. Curve 1 in this figure is given for comparison. It shows the dependence $\lambda^{-2}(T)$ in the absence of Coulomb interactions ($U_p = V_1 = V_2 = 0$). The remaining curves demonstrate modification of the temperature dependence of λ^{-2} with successive switching on the interactions. Note that the parameter V_1 , as was said above, does not enter the set of equations for order parameter (16) [52] and, therefore, does not affect the function $\lambda^{-2}(T)$. Curve 2 is obtained by take into account the interactions between the second neighbors; curve 3—only the Hubbard repulsion; and curve 4—both types of interaction. It is seen that the effect of the Coulomb interaction, in full agreement with the results of [32, 55], is manifested in a significant decrease in the critical temperature of the transition to the superconducting phase. The resulting

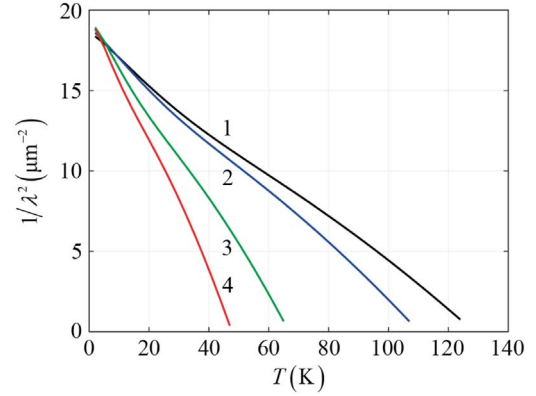


Figure 2. The effect of Coulomb repulsion on the temperature dependence of inverse square of the London penetration depth in the SFM of cuprate HTSCs. Curve 1 is calculated with the value of the Coulomb interaction parameters $U_p = V_2 = 0$; curve 2—for $U_p = 0$, $V_2 = 0.1$ eV; curve 3—for $U_p = 3$ eV, $V_2 = 0$; curve 4—for $U_p = 3$ eV, $V_2 = 0.1$ eV. The value of V_1 is not specified since according to (16) it does not contribute to the d-wave pairing in the SFM. The other model parameter are (in eV): $\tau = 0.225$, $t = 0.12$, $J = 1.76$, $I = 0.12$ and $\alpha_x = 0.002$, $x = 0.17$.

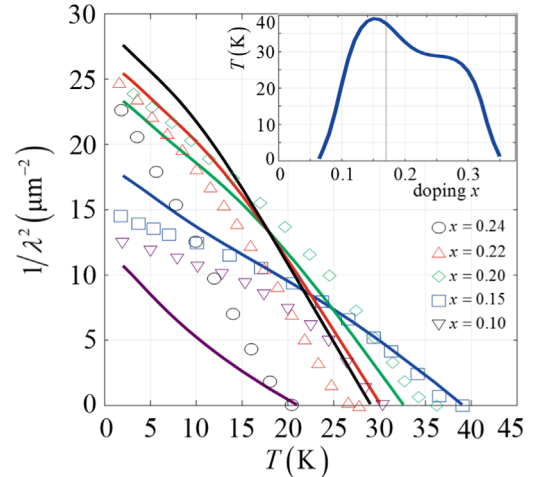


Figure 3. Temperature dependence of the inverse square of the London penetration depth at five doping levels. The solid curves are calculated theoretically. The symbolic curves are taken from experimental work on $\text{La}_{2-x}\text{Sr}_x\text{CuO}_4$ [31]. Matching to one level of doping for solid and symbolic curves is indicated by the same color. The magnitudes of doping x are indicated next to corresponding symbols. The insert shows doping dependence of the critical temperature. The model parameters (in eV): $\tau = 0.225$, $t = 0.12$, $J = 1.76$, $I = 0.118$, $U_p = 3.3$, $V_2 = 0.1$. V_1 is not specified since it does not contribute to d-wave pairing in the SFM. The phase: $\alpha_x = 0.002$.

decrease in T_c allows us to achieve a much better agreement of the calculated temperature dependencies of λ^{-2} with the experimental data. Figure 3 compares the temperature dependencies of λ^{-2} obtained at different doping within the SFM model (solid lines) with that taken from the experiment on $\text{La}_{2-x}\text{Sr}_x\text{CuO}_4$ [31] (symbolic curves). The T_c-x phase diagram, shown in the insert, is obtained within the spin-polaron approach and correlates well to the experimental phase diagram for LSCO superconductors in both the left boundary of the superconducting dome at $x \cong 0.05$ and the

maximum critical temperature $T_{\max} = 39$ K. At the same time, the right boundary of the theoretical dome exceeds that of experimental dome by the value of about 0.1. The reason for this is that in the present study, we adopted the low-density approximation, and hence in the strongly overdoped regime our theory seems to be insufficient. As a result a theoretical curve $\lambda^{-2}(T)$ for large doping $x = 0.24$ significantly differs from the experimental one since in real LSCO at $x = 0.24$ the critical temperature $T_c = 20$ K, but according to the phase diagram shown in the insert $T_c = 30$ K.

A comparison of the temperature curves of λ^{-2} for the same doping x in the figure 3 shows that the values of T_c and $\lambda^{-2}(T=0)$ are on the whole well reproduced for $x = 0.15$ – 0.22 . It can be seen from the figure that all the theoretical temperature dependencies $\lambda^{-2}(T)$, except for $x = 0.10$, are slightly convex, as in most experiments on cuprate superconductors [26, 28, 31]. For the doping level $x = 0.10$ (the lowest solid curve in the figure 3) the form of $\lambda^{-2}(T)$ is concave over the entire temperature range what seems to be incompatible with corresponding experimental curve measured in [31]. This discrepancy is most likely due to the strong spin-charge fluctuations which are well developed in the strongly underdoped regime and which, in particular, result in pseudogap (PG) behavior in cuprates. The present theory is, however, a mean field theory, it does not take into account these spin-charge fluctuations and therefore PG behavior. Since, however, the PG is weak at optimal and higher doping $x \geq 0.15$, we are confident that our results for $x = 0.15$ – 0.22 will be unaffected by the PG behavior.

The comparison of the calculated temperature dependencies $\lambda^{-2}(T)$ on figure 3 with the corresponding curves from our previous paper [25] leads to the conclusion that the main effect of taking into account the Coulomb interaction is the decrease of T_c . It is important that the main result of [25], the inflection point associated with the change of curvature of the function $\lambda^{-2}(T)$ and found experimentally in a number of compounds [26–30, 56] remained unaffected. This inflection point was considered as a confirmation of the spin-polaron concept of quasiparticles in cuprate HTSCs.

7. Conclusion

Within the spin polaron concept, the effect of Coulomb repulsion on modification of the temperature dependence of the London penetration depth λ in cuprate high-temperature superconductors was studied.

When obtaining expressions for calculating λ two types of Coulomb interactions were taken into account: (1) Hubbard repulsion of two holes on one site and (2) Coulomb repulsion of two holes located on the next-nearest-neighbor oxygen ions. The interaction of the holes on the nearest-neighbor sites was not taken into account because, according to the results of [52], it does not contribute to the d-wave superconductivity within spin-fermion model.

The calculation of the London penetration depth λ was carried out on the basis of the method developed by the authors in [25] in the framework of the spin-polaron approach, which takes into account the strong coupling between the charge and spin degrees of freedom, as well as the real structure of the CuO_2 -planes with two oxygen ions per unit cell.

On the basis of numerical calculations of the temperature dependence of inverse square of the London penetration depth, carried out with the generally accepted values of the Emery model parameters, it was shown that taking into account the Coulomb interaction results in, as expected from [32, 55], a significant decrease in the critical temperature corresponding to zeros of the function $\lambda^{-2}(T)$. This circumstance enabled one to achieve substantially better agreement of the theoretical curves with experimental results [31], in rather broad range for x around optimal doping ($x = 0.15$, 0.20 and 0.22). At the same time for strongly overdoped and underdoped compounds our results for $\lambda^{-2}(T)$ reveal discrepancy with experimental data. We argue that for large doping ($x = 0.24$) this discrepancy is because in our theory the low-density approximation was adopted and hence for doping as large as $x = 0.24$ this approximation may be insufficient. On the other hand, the strong spin-charge fluctuations, which in the low doping regime are well developed due to proximity to antiferromagnetic region, are not taken into account properly in our theory. We suggest this to be the main reason for discrepancy of our results for $\lambda^{-2}(T)$ with experimental one at doping as small as $x = 0.10$.

However, for cuprates with moderate doping $x = 0.15$, 0.20 , and 0.22 the proposed theory describes the experimental dependencies $\lambda^{-2}(T)$ quite well and clearly shows that accounting for the Coulomb interaction leads to an almost three-fold decrease in the value of T_c , but does not change the functional form of the temperature dependence of λ^{-2} , which was obtained earlier. In particular, the inflection point of the function $\lambda^{-2}(T)$, whose existence is considered by us as a confirmation of the spin-polaron nature of the quasiparticles in cuprates, remained intact.

Acknowledgments

The work was financially supported by the Russian Foundation for Basic Research (project #18-02-00837, #20-32-70059), the Government of Krasnoyarsk Region, the Krasnoyarsk Regional Science and Technology Support Fund (projects: #18-42-240014 ‘One-orbit effective model of an ensemble of spin-polaron quasiparticles in the problem of describing the intermediate state and pseudogap behavior of cuprate superconductors’ and #18-42-243002 ‘Manifestation of spin-nematic correlations in spectral characteristics of electronic structure and their influence on practical properties of cuprate superconductors’). The work of KKK was supported by the Council for Grants of the President of the Russian Federation (project MK-1641.2020.2).

Appendix

A.1. Digitized Film Strips

The equations for the components of the superconducting order parameter, which are discussed at the beginning of the section 5, have the form

$$\begin{aligned} \Delta_{1k} &= -(\cos k_x - \cos k_y) \frac{2V_2}{N} \sum_q \cos q_x \langle a_{q\uparrow} a_{-q\downarrow} \rangle, \\ \Delta_{4k} &= -(\cos k_x - \cos k_y) \frac{2V_2}{N} \sum_q \cos q_x \langle b_{q\uparrow} b_{-q\downarrow} \rangle, \\ \Delta_{5k} &= +(\cos k_x - \cos k_y) \frac{I}{N} \sum_q (\cos q_x - \cos q_y) \\ &\quad \times (\langle L_{q\uparrow} L_{-q\downarrow} \rangle - C_1 \langle u_{q\uparrow} u_{-q\downarrow} \rangle) \\ &\quad + \frac{U_p}{N} \sum_q \frac{C_1}{2} (\cos k_x - 2\alpha_x) \langle a_{q\uparrow} a_{-q\downarrow} \rangle \\ &\quad + \cos k_y \langle b_{q\uparrow} b_{-q\downarrow} \rangle \\ &\quad - (\cos k_x - \cos k_y) \frac{V_2}{N} \sum_q C_1 \cos q_x \\ &\quad \times (\langle a_{q\uparrow} a_{-q\downarrow} \rangle + \langle b_{q\uparrow} b_{-q\downarrow} \rangle), \end{aligned} \quad (\text{A.1})$$

where

$$\begin{aligned} \langle u_{q\uparrow} u_{-q\downarrow} \rangle &= -s_{q,x}^2 \langle a_{q\uparrow} a_{-q\downarrow} \rangle - s_{q,y}^2 \langle b_{q\uparrow} b_{-q\downarrow} \rangle \\ &\quad - s_{q,x} s_{q,y} (\langle a_{q\uparrow} b_{-q\downarrow} \rangle + \langle b_{q\uparrow} a_{-q\downarrow} \rangle). \end{aligned} \quad (\text{A.2})$$

Functions $S_{ij}^{(l)}(k, \omega)$ used when writing expressions (18) are defined as

$$\begin{aligned} S_{11}^{(1)}(k, \omega) &= +Q_{3y}(k, -\omega) Q_{3y}(k, \omega), \\ S_{21}^{(1)}(k, \omega) &= +S_{12}^{(1)}(k, -\omega) = Q_3(k, -\omega) Q_{3y}(k, \omega), \\ S_{11}^{(4)}(k, \omega) &= +S_{22}^{(1)}(k, \omega) = Q_3(k, -\omega) Q_3(k, \omega), \\ S_{11}^{(5)}(k, \omega) &= -Q_y(k, -\omega) Q_y(k, \omega), \\ S_{12}^{(4)}(k, \omega) &= +Q_3(k, -\omega) Q_{3x}(k, \omega), \\ S_{21}^{(4)}(k, \omega) &= +S_{12}^{(4)}(k, -\omega), \\ S_{12}^{(5)}(k, \omega) &= -Q_y(k, -\omega) Q_x(k, \omega), \\ S_{21}^{(5)}(k, \omega) &= +S_{12}^{(5)}(k, -\omega), \\ S_{22}^{(4)}(k, \omega) &= +Q_{3x}(k, -\omega) Q_{3x}(k, \omega), \\ S_{22}^{(5)}(k, \omega) &= -Q_x(k, -\omega) Q_x(k, \omega), \\ S_{33}^{(1)}(k, \omega) &= -K_k^2 S_{11}^{(5)}(k, \omega), \\ S_{33}^{(4)}(k, \omega) &= +K_k^2 S_{22}^{(5)}(k, \omega), \\ S_{33}^{(5)}(k, \omega) &= +Q_{xy}(k, -\omega) Q_{xy}(k, \omega), \end{aligned} \quad (\text{A.3})$$

where

$$\begin{aligned} Q_{x(y)}(k, \omega) &= (\omega - \xi_{x(y)}) J_{y(x)} + t_k J_{x(y)}, \\ Q_3(k, \omega) &= (\omega - \xi_L) t_k + J_x J_y K_k, \\ Q_{3x(3y)}(k, \omega) &= (\omega - \xi_L)(\omega - \xi_{x(y)}) - J_{x(y)}^2 K_k, \\ Q_{xy}(k, \omega) &= (\omega - \xi_x)(\omega - \xi_y) - t_k^2. \end{aligned} \quad (\text{A.4})$$

The function $R^x(k, \omega)$, which is included in the equation for the chemical potential (23), is defined as follows

$$\begin{aligned} R^x(k, \omega) &= (Q_{3y}(k, \omega) + Q_{3x}(k, \omega)) \Psi(k, \omega) \\ &\quad - 2(J_x Q_y(k, -\omega) \Delta_{1k}^* + J_y Q_x(k, -\omega) \Delta_{4k}^*) \Delta_{5k}^* \\ &\quad - (\omega - \xi_L)(Q_{3y}(k, -\omega) \Delta_{1k}^{*2} + Q_{3x}(k, -\omega) \Delta_{4k}^{*2}) \\ &\quad - (2\omega - \xi_x - \xi_y) Q_{xy}(k, -\omega) \Delta_{5k}^{*2} / K_k^2, \end{aligned} \quad (\text{A.5})$$



$$\Psi(k, \omega) = (\omega + E_k)(\omega + \epsilon_{2,-k})(\omega + \epsilon_{1,-k}). \quad (\text{A.6})$$

Thermodynamic averages of equation (10) are defined by the expressions

$$\begin{aligned} \langle a_{k\alpha}^\dagger a_{k\alpha} \rangle &= Q_{3y}(k, \omega) \Psi(k, \omega) - 2J_y Q_x(k, -\omega) \Delta_{4k}^* \Delta_{5k}^* \\ &\quad - (\omega - \xi_L) Q_{3x}(k, -\omega) \Delta_{4k}^{*2} \\ &\quad - (\omega - \xi_y) Q_{xy}(k, -\omega) \Delta_{5k}^{*2} / K_k^2, \\ \langle a_{k\alpha}^\dagger b_{k\alpha} \rangle &= Q_3(k, \omega) \Psi(k, \omega) + J_x Q_x(k, -\omega) \Delta_{4k}^* \Delta_{5k}^* \\ &\quad + J_y Q_y(k, -\omega) \Delta_{1k}^* \Delta_{5k}^* - t_k Q_{xy}(k, -\omega) \Delta_{5k}^{*2} / K_k^2 \\ &\quad + (\omega - \xi_L) Q_3(k, -\omega) \Delta_{1k}^* \Delta_{4k}^*, \\ \langle a_{k\alpha}^\dagger L_{k\alpha} \rangle &= Q_y(k, \omega) K_k \Psi(k, \omega) + t_k Q_x(k, -\omega) \Delta_{4k}^* \Delta_{5k}^* \\ &\quad + J_y Q_3(k, -\omega) K_k \Delta_{1k}^* \Delta_{4k}^* - J_x Q_{3x}(k, -\omega) K_k \Delta_{4k}^{*2} \\ &\quad + (\omega - \xi_y) Q_y(k, -\omega) \Delta_{1k}^* \Delta_{5k}^*, \end{aligned} \quad (\text{A.7})$$

where $\Psi(k, \omega)$ is defined in (A.6).

ORCID iDs

K K Komarov  <https://orcid.org/0000-0001-9330-879X>
 D M Dzebisashvili  <https://orcid.org/0000-0002-0402-1947>

References

- [1] Emery V J 1987 *Phys. Rev. Lett.* **58** 2794
- [2] Varma C M, Schmitt-Rink S and Abrahams E 1987 *Solid State Commun.* **62** 681
- [3] Hirsch J E 1987 *Phys. Rev. Lett.* **59** 228
- [4] Gaididei Y B and Loktev V M 1988 *Phys. Status Solidi B* **147** 307
- [5] Ovchinnikov S G and Sandalov I S 1989 *Physica C* **161** 607
- [6] Barabanov A F, Maksimov L A and Uimin G V 1988 *JETP Lett.* **47** 622
- [7] Zaanen J and Oleš A M 1988 *Phys. Rev. B* **37** 9423
- [8] Emery V J and Reiter G 1988 *Phys. Rev. B* **38** 4547
- [9] Prelovšek P 1988 *Phys. Lett. A* **126** 287
- [10] Stechel E B and Jennison D R 1988 *Phys. Rev. B* **38** 4632
- [11] Kohno M 2018 *Rep. Prog. Phys.* **81** 042501
- [12] Kitatani M, Schafer T, Aoki H and Held K 2019 *Phys. Rev. B* **99** 041115(R)
- [13] Spalek J, Zegrodnik M and Kaczmarczyk J 2017 *Phys. Rev. B* **95** 024506
- [14] Barabanov A F, Maksimov L A and Zhukov L E 1993 *Physica C* **212** 375
- [15] Barabanov A F, Berezovskii V M, Zasinias E and Maksimov L A 1996 *JETP* **83** 819

- [16] Barabanov A F, Kuzian R O and Maksimov L A 1997 *Phys. Rev. B* **55** 4015
- [17] Starykh O A, de Alcantara Bonfim O F and Reiter G F 1995 *Phys. Rev. B* **52** 12534
- [18] Barabanov A F, Zasinan E, Urazaev O V and Maksimov L A 1997 *JETP Lett.* **66** 182
- [19] Barabanov A F, Kovalev A A, Urazaev O V, Belemuk A M and Hayn R 2001 *JETP* **92** 677
- [20] Kuzian R O, Hayn R and Barabanov A F 2003 *Phys. Rev. B* **68** 195106
- [21] Dzebisashvili D M, Val'kov V V and Barabanov A F 2013 *JETP Lett.* **98** 528
- [22] Val'kov V V, Dzebisashvili D M and Barabanov A F 2015 *Phys. Lett. A* **379** 421
- [23] Val'kov V V, Dzebisashvili D M and Barabanov A F 2015 *J. Low Temp. Phys.* **181** 134
- [24] Val'kov V V, Dzebisashvili D M and Barabanov A F 2016 *J. Supercond. Nov. Magn.* **29** 1049
- [25] Dzebisashvili D M and Komarov K K 2018 *Eur. Phys. J. B* **91** 278
- [26] Khasanov R, Shengelaya A, Maisuradze A, Mattina F L, Bussmann-Holder A, Keller H and Muller K A 2007 *Phys. Rev. Lett.* **98** 057007
- [27] Wojek B M, Weyeneth S, Bosma S, Pomjakushina E and Puzniak R 2011 *Phys. Rev. B* **84** 144521
- [28] Sonier J E, Brewer J H, Kiefl R F, Morris G D, Miller R I, Bonn D A, Chakhalian J, Heffner R H, Hardy W N and Liang R 1999 *Phys. Rev. Lett.* **83** 4156
- [29] Khasanov R, Strassel S, Castro D D, Masui T, Miyasaka S, Tajima S, Bussmann-Holder A and Keller H 2007 *Phys. Rev. Lett.* **99** 237601
- [30] Anukool W, Barakat S, Panagopoulos C and Cooper J R 2009 *Phys. Rev. B* **80** 024516
- [31] Panagopoulos C, Rainford B D, Cooper J R, Lo W, Tallon J L, Loram J W, Betouras J, Wang Y S and Chu C W 1999 *Phys. Rev. B* **60** 14617
- [32] Val'kov V V, Dzebisashvili D M, Korovushkin M M and Barabanov A F 2017 *JETP* **125** 810
- [33] Hybertsen M S, Schluter M and Christensen N E 1989 *Phys. Rev. B* **39** 9028
- [34] Ogata M and Fukuyama H 2008 *Rep. Prog. Phys.* **71** 036501
- [35] Fischer M H and Kim E-A 2011 *Phys. Rev. B* **84** 144502
- [36] Val'kov V V, Dzebisashvili D M, Korovushkin M M and Barabanov A F 2017 *Magn. Magn. Mat.* **440** 123
- [37] Barabanov A F, Mikheenkova A V and Shvartsberg A V 2011 *Theor. Math. Phys.* **168** 1192
- [38] Shimahara H and Takada S 1991 *JPSJ* **60** 2394
- [39] Peierls R 1933 *Z. Physik* **80** 763
- [40] Lifshitz E M and Pitaevskii L P 1980 *Statistical Physics: Theory of the Condensed State (Part, 2)* (Oxford: Pergamon) p 387
- [41] Schrieffer J R 1964 *Theory of Superconductivity* (New York: Benjamin) p 332
- [42] Tinkham M 1996 *Introduction to Superconductivity* (New York: McGraw-Hill) p 454
- [43] Zwanzig R 1961 *Phys. Rev.* **124** 983
- [44] Mori H 1965 *Prog. Theor. Phys.* **33** 423
- [45] Roth L M 1968 *Phys. Rev. Lett.* **20** 1431
- [46] Roth L M 1969 *Phys. Rev.* **184** 451
- [47] Rowe D J 1968 *Rev. Mod. Phys.* **40** 153
- [48] Tserkovnikov Y A 1981 *Teor. Mat. Fiz.* **49** 219
Tserkovnikov Y A 1982 *Theoretical and Mathematical Physics* **52** 712
- [49] Plakida N M 2010 *High-Temperature Cuprate Superconductors* (Berlin: Springer) p 570
- [50] Mancini F and Avella A 2004 *Adv. Phys.* **53** 537
- [51] Izyumov Y A 1999 *Phys. Usp.* **42** 215
- [52] Val'kov V V, Dzebisashvili D M, Korovushkin M M and Barabanov A F 2016 *JETP Lett.* **103** 385
- [53] Zubarev D N 1960 *Sov. Phys. Usp.* **3** 320
- [54] Val'kov V V, Dzebisashvili D M, Korovushkin M M, Komarov K K and Barabanov A F 2019 *JETP* **128** 885
- [55] Val'kov V V, Dzebisashvili D M, Korovushkin M M and Barabanov A F 2018 *J. Low Temp. Phys.* **191** 408
- [56] Howald L *et al* 2018 *Phys. Rev. B* **97** 094514